Robotica (2009) volume 27, pp. 961–969. © Cambridge University Press 2009
doi:10.1017/S0263574709005384

Kinematic analysis of a fully decoupled translational parallel manipulator

M. Ruggiu*

Department of Mechanical Engineering, University of Cagliari, Piazza d'Armi – 09123 Cagliari, Italy

(Received in Final Form: January 26, 2009. First published online: February 27, 2009)

SUMMARY

The paper describes the kinematic analysis of a new translational parallel manipulator (TPM). The manipulator consists of a fixed base, with a moving platform connected to the base by three identical legs with PUPR chains. The axes of the actuated motions are orthogonal. This configuration provides a very simplified kinematic analysis with fully decoupled input–output linear equations, absence of translational singularities, isotropy and ease of determining the workspace for the moving platform.

KEYWORDS: Parallel mechanism; Translational parallel manipulator; Singularities; Workspace.

1. Introduction

Manipulators with 3 degrees of freedom (DOF) in translation may find numerous applications in industry like in pick and place operations or machining. Hence they are an important research subject for the robotic community. In comparison with the full mobility parallel manipulators, the complexity of the kinematics and dynamics relationships of the minor mobility manipulators are dramatically reduced, thereby allowing for a simpler analysis and control. The first translational parallel manipulator (TPM) to be proposed was the *Delta* robot of Clavel,[1] which was based on the RRP_aR architecture of each leg. R stands for revolute pair, P_a for parallelogram structure. Several variants of the *Delta* robot were proposed. Either the *Linear Delta*, or the *Triax* by Sheldon replace the revolute motor and lever with a linear actuator. Another interesting robot was the *Orthoglide*[2] developed for machine-tool application with the PRP_aR architecture of each leg (P stands for prismatic). Also the *Tricept*[3] robot is successful as a machine tool. Its architecture is somewhat hybrid and complex with a stem connecting the end-effector to the base through 2U pairs (U stands for universal) and three legs with RRPS chains.

Very numerous scientific works deal with the 3UPU architecture,[4,5] first proposed by Tsai, which is a special case of the family of 3RRPRR mechanisms and with some of its variants, namely 3PUU, 3RUU.[6] The 3UPU architecture was proved to be very sensitive to the manufacturing tolerance and exhibits rotational singularities. This problem seems to be overcome by Carricato and Parenti Castelli[7,8,9] with the 3PRRRR. However, great interest has been focused on these manipulators because each leg preserves 5-DOF producing not-overconstrained manipulators. A robot with the 3RCC (3CCR) architecture belongs to this class of TPMs as well. Examples of TPMs exhibiting 4-DOF for each leg are less in number. Gosselin *et al*. proposed the *Tripteron* with fully decoupled linear input–output equations[10] and Gosselin and Kong proposed the 3CRR and some of its variants.[11]

There is an extensive work of synthesis underpinning these designs for TPMs. Hervé[12] deals with the displacement group theory; Gosselin and Kong proposed a systematic approach based on the screw theory.[13,14] Among others, the work done by Carricato and Parenti Castelli[7] and Frisoli *et al.*[15] is noteworthy. Staicu *et al.*[16,17] proposed a recursive matrix method in order to express the kinematics and dynamics relationships of the 3-DOF parallel manipulators. This method of analysis seems to be very attractive and efficient for the TPMs.

This paper proposes a novel not-overconstrained TPM, a variant of the 3RRPRR mechanism. Each leg is composed of the PUPR architecture with the P pairs connected to the base actuated and having orthogonal directions. This architecture provides a very simple, fully decoupled input–output kinematic relationships. Although the proposed TPM belongs to a class of manipulators whose geometrical synthesis was extensively developed and even the specific PUPR sequence of pairs for leg is included in a table of ref. [13], no works were found by the author developing the full analysis of the kinematics of such manipulator. The orthogonal arrangement of the motor axes proposed in the paper has the merit of simplifying the kinematics and therefore the control of the robot; the presence of two P pairs for each leg allows the moving platform to reach a wide workspace. In a prototype, the mechanism can also be implemented by a spatial 3-DOF manipulator of type PRPR. In the author's opinion, therefore, the paper presents an original contribution and practical interest.

The paper is categorised as follows: first, the geometric description of the TPM is given. Then, the mobility analysis is performed, which proves that the moving platform does not rotate. The position analysis with the inverse and forward kinematics are dealt with in Section 4. Section 5 is dedicated to the velocity analysis, Jacobian matrix and singularity issues. In Section 6, a numerical simulation of the kinematics of the passive joints in a leg is proposed. In Section 7, the workspace of the TPM is obtained by the geometrical approach. Section 8 shows two alternative designs of the TPM with the P pair directions forming either $2\pi/3$ or

* Corresponding author. E-mail: ruggiu@dimeca.unica.it

https://doi.org/10.1017/S0263574709005384 Published online by Cambridge University Press

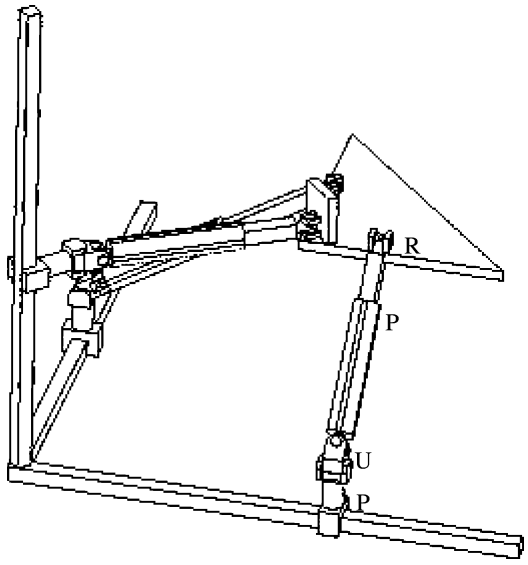


Fig. 1. The PUPR parallel manipulator.

$\pi/2$. Simple kinematics relationships were deduced for these architectures as well. In Section 8, as well, a design of the PUPR free from any singularities is proposed. Finally, the conclusions are drawn.

2. Geometry of the TPM

The TPM consists of a fixed base and a moving platform, shaped as a right triangle, connected to the base by three identical legs (Fig. 1). Each leg consists of three rigid links connected to each other by a universal (U) and a prismatic (P) joint. The leg is either connected to the base by a prismatic pair (P) or to the moving platform by a revolute pair (R). The axes of the prismatic pairs connected to the base are orthogonal. Further, the P pair, connecting the leg to the base, and the first axis of the successive U pair are to be parallel.

3. Mobility Analysis

With reference to Fig. 2, in order to study the kinematics of the present TPM, some local reference systems are assigned travelling the ith leg. A fixed reference system O-xyz with origin at the intersection of the prismatic axes and a mobile reference system P-$x_P y_P z_P$ superimposed on to the moving platform were assigned. The reference System 1i is obtained from the fixed reference system by a rotation through ϕ_i about z followed by a rotation through α_i about $\hat{\mathbf{y}}_{1i}$ and then an a_i translation along $\hat{\mathbf{x}}_{1i}$. The second reference system 2i is obtained by a rotation through ϑ_i about $\hat{\mathbf{x}}_{1i}$. The third reference system 3i is obtained by a rotation through χ_i about $\hat{\mathbf{y}}_{2i}$. The b_i linear motion along $\hat{\mathbf{z}}_{3i}$ makes up the fourth reference system. Finally, the fifth reference system is obtained by a rotation through λ_i about $\hat{\mathbf{x}}_{4i}$.

By a constant displacement l_i on the moving platform and two successive rotations of $-\alpha_i$ and $-\phi_i$ about the actual axes $\hat{\mathbf{y}}_{5i}$ and $\hat{\mathbf{z}}_{6i}$, respectively, the system P-$x_P y_P z_P$ is located on the mobile platform parallel to the fixed reference system.

In the present PUPR parallel platform, the constant angles ϕ_i and α_i $(i = 1, 2, 3)$ are $\phi_1 = 0$, $\phi_2 = \pi/2$, $\phi_3 = -3\pi/4$, $\alpha_1 = 0$, $\alpha_2 = 0$, $\alpha_3 = -\pi/2$ (Fig. 2).

The orientation matrix ${}^0\mathbf{R_P}$ of the moving platform with respect to the fixed reference system O-xyz is given by the identity matrix for every configuration assumed by the TPM. ${}^0\mathbf{R_P}$ may be expressed as the subsequent rotations of the reference systems attached to leg i from O-xyz to P-$x_P y_P z_P$.

$$
\begin{aligned}
{}^0\mathbf{R_P} = \mathbf{R_z}(\phi_i) \cdot \mathbf{R}_{\hat{\mathbf{y}}_{1i}}(\alpha_i) \cdot \mathbf{R}_{\hat{\mathbf{x}}_{2i}}(\vartheta_i) \cdot \mathbf{R}_{\hat{\mathbf{y}}_{3i}}(\chi_i) \cdot \mathbf{R}_{\hat{\mathbf{x}}_{4i}}(\lambda_i) \\
\cdot \mathbf{R}_{\hat{\mathbf{y}}_{5i}}(-\alpha_i) \cdot \mathbf{R}_{\hat{\mathbf{z}}_{6i}}(-\phi_i) = \mathbf{I}, \qquad (1)
\end{aligned}
$$

where $\mathbf{I}$ indicates the identity matrix, $\mathbf{R_z}$, $\mathbf{R_y}$, $\mathbf{R_x}$ are the three basic rotation matrices about z, y, x, respectively. For each ith leg, an $\mathbf{R}_{jj}$ term is $\cos(\chi_i) = c(\chi_i) = 1$, such that $\chi_i = 0$ and a $\mathbf{R}_{ij}$ $(i \neq j)$ term is $s(\vartheta_i) \cdot c(\lambda_i) + s(\lambda_i) \cdot c(\vartheta_i) = s(\vartheta_i + \lambda_i) = 0$, such that $(\vartheta_i + \lambda_i) = 0$. Therefore, assembling the platform such that $\chi_i = 0$ and $(\vartheta_i + \lambda_i) = 0$ always yields to a moving platform parallel to the base.

In order to prove that the moving platform never rotates its angular velocity $\boldsymbol{\omega}$ may be expressed as a sum of the joint rates in the ith leg

$$
\boldsymbol{\omega} = \dot{\vartheta}_i \hat{\mathbf{x}}_{2i} + \dot{\chi}_i \hat{\mathbf{y}}_{3i} + \dot{\lambda}_i \hat{\mathbf{x}}_{4i}, \qquad (2)
$$

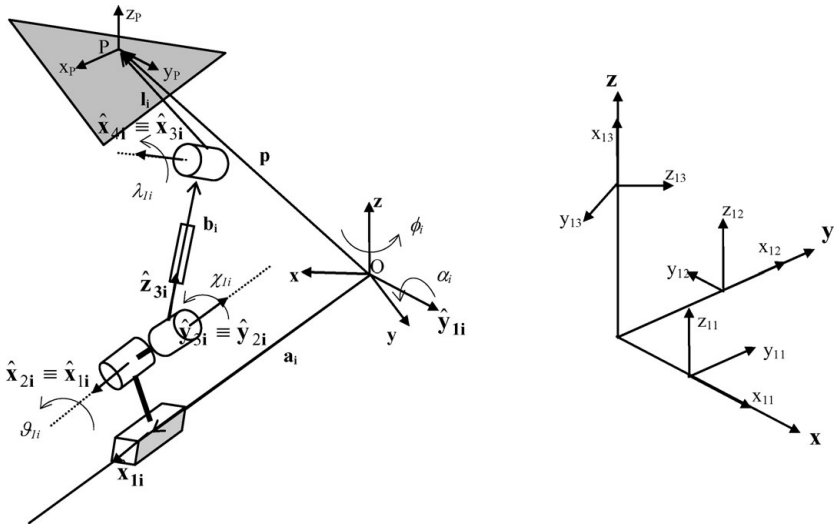


Fig. 2. The ith leg of the TPM.

https://doi.org/10.1017/S0263574709005384 Published online by Cambridge University Press

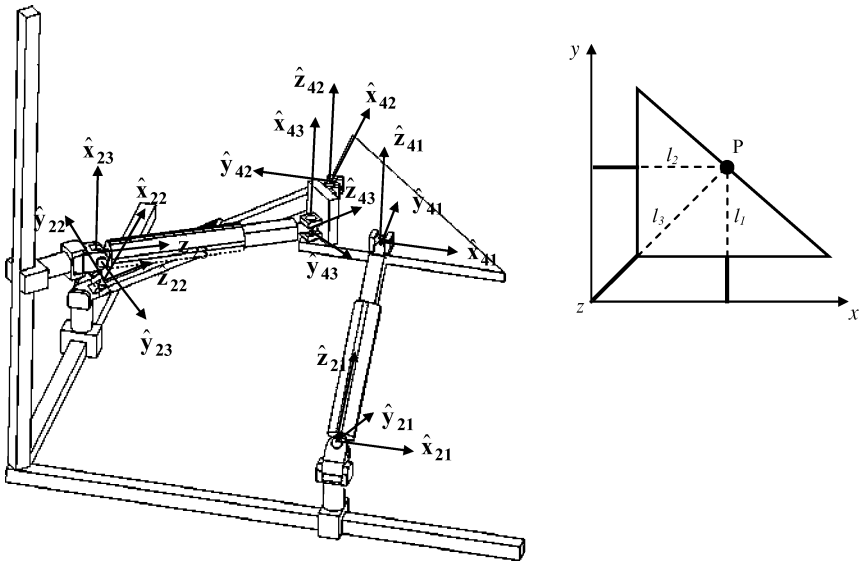


Fig. 3. The local frames setting.

where

$$\hat{\mathbf{x}}_{2i} = \mathbf{R}_{\mathbf{z}}(\phi_i)\mathbf{R}_{\hat{\mathbf{y}}_{1i}}(\alpha_i)\begin{pmatrix}1\\0\\0\end{pmatrix};$$

$$\hat{\mathbf{y}}_{3i} = \mathbf{R}_{\mathbf{z}}(\phi_i)\mathbf{R}_{\hat{\mathbf{y}}_{1i}}(\alpha_i)\mathbf{R}_{\hat{\mathbf{x}}_{2i}}(\vartheta_i)\begin{pmatrix}0\\1\\0\end{pmatrix};$$

$$\hat{\mathbf{x}}_{4i} = \mathbf{R}_{\mathbf{z}}(\phi_i)\mathbf{R}_{\hat{\mathbf{y}}_{1i}}(\alpha_i)\mathbf{R}_{\hat{\mathbf{x}}_{2i}}(\vartheta_i)\mathbf{R}_{\hat{\mathbf{y}}_{3i}}(\chi_i)\begin{pmatrix}1\\0\\0\end{pmatrix}. \tag{3}$$

Considering the relationships between the passive angles, the Cartesian components of the angular velocity $\boldsymbol{\omega}$ may be expressed as follows:

$$\begin{aligned}\omega_x &= -c\alpha_i c\phi_i \cdot (\dot{\vartheta}_i + \dot{\lambda}_i) + (s\phi_i c\vartheta_i + c\phi_i c\alpha_i s\vartheta_i)\cdot \dot{\chi}_i\\ \omega_y &= s\alpha_i s\phi_i \cdot (\dot{\vartheta}_i + \dot{\lambda}_i) + (c\phi_i c\vartheta_i + s\phi_i s\alpha_i s\vartheta_i)\cdot \dot{\chi}_i\\ \omega_z &= -s\alpha_i \cdot (\dot{\vartheta}_i + \dot{\lambda}_i) + c\alpha_i s\vartheta_i \cdot \dot{\chi}_i\end{aligned} \tag{4}$$

Writing out ω_x, ω_y, ω_z for $i = 1,2,3$ and equating them, the following set of equations is deduced:

$$\begin{array}{lll}(\omega_x)_1 = (\omega_x)_3 & (\omega_x)_1 = (\omega_x)_2 & (\omega_x)_2 = (\omega_x)_3\\ -(\dot{\vartheta}_1 + \dot{\lambda}_1) + s\vartheta_1 \cdot \dot{\chi}_1 = 0 & -(\dot{\vartheta}_1 + \dot{\lambda}_1) + s\vartheta_1 \cdot \dot{\chi}_1 & c\vartheta_2 \cdot \dot{\chi}_2 = 0\\ & = c\vartheta_2 \cdot \dot{\chi}_2 & \\ (\omega_y)_1 = (\omega_y)_3 & (\omega_y)_1 = (\omega_y)_2 & (\omega_y)_2 = (\omega_y)_3\\ c\vartheta_1 \cdot \dot{\chi}_1 = c\vartheta_3 \cdot \dot{\chi}_3 & c\vartheta_1 \cdot \dot{\chi}_1 = 0 & 0 = c\vartheta_3 \cdot \dot{\chi}_3\\ (\omega_z)_1 = (\omega_z)_3 & (\omega_z)_1 = (\omega_z)_2 & (\omega_z)_2 = (\omega_z)_3\\ s\vartheta_1 \cdot \dot{\chi}_1 = (\dot{\vartheta}_3 + \dot{\lambda}_3) & s\vartheta_1 \cdot \dot{\chi}_1 = (\dot{\vartheta}_2 + \dot{\lambda}_2) & (\dot{\vartheta}_2 + \dot{\lambda}_2) = (\dot{\vartheta}_3 + \dot{\lambda}_3)\end{array} \tag{5}$$

Using six equations of the set of nine equations leads to a homogeneous algebraic system of six unknowns $(\dot{\vartheta}_i + \dot{\lambda}_i)$, $\dot{\chi}_i$ $(i = 1, 2, 3)$ whose only admissible solution is

$$(\dot{\vartheta}_i + \dot{\lambda}_i) = \dot{\chi}_i = 0. \tag{6}$$

Substituting Eqs. (6) into Eqs. (4), it is obtained that $\omega_x = \omega_y = \omega_z = 0$, thus proving that the moving platform does not rotate. Since the proof of the translational motion of the platform is valid for any configuration assumed by the manipulator and thus for any time, it is guaranteed that the moving platform never starts rotating, i.e. $\dot{\omega} = 0$.

4. Position Analysis

With reference to Fig. 2, the loop closure equation for the ith leg may be readily written as

$${}^{1i}\mathbf{a}_i + {}^{3i}\mathbf{b}_i + {}^{4i}\mathbf{l}_i = {}^{0}\mathbf{p}. \tag{7}$$

Vectors of Eq. (7) are to be expressed in a common reference. For simplicity the reference system of the actuated variable a_i is used.

$${}^{1i}\mathbf{a}_i + {}^{1i}\mathbf{R}_{3i}\,{}^{3i}\mathbf{b}_i + {}^{1i}\mathbf{R}_{4i}\,{}^{4i}\mathbf{l}_i = {}^{1i}\mathbf{R}_0\,{}^{0}\mathbf{p}. \tag{8}$$

Considering that $\chi_i = 0$ and $(\vartheta_i + \lambda_i) = 0$, the terms of Eq. (8) assume a very simplified form

$$\begin{aligned}{}^{1i}\mathbf{R}_{3i} &= {}^{1i}\mathbf{R}_{2i}\,{}^{2i}\mathbf{R}_{3i} = \mathbf{R}_{\hat{\mathbf{x}}_{1i}}(\vartheta_i)\mathbf{I}\\ {}^{1i}\mathbf{R}_{4i} &= {}^{1i}\mathbf{R}_{2i}\,{}^{2i}\mathbf{R}_{3i}\,{}^{3i}\mathbf{R}_{4i} = \mathbf{R}_{\hat{\mathbf{x}}_{1i}}(\vartheta_i)\mathbf{I}\mathbf{R}_{\hat{\mathbf{x}}_{3i}}(\lambda_i)\\ &= \mathbf{R}_{\hat{\mathbf{x}}_{1i}}(\vartheta_i + \lambda_i) = \mathbf{I}\\ {}^{1i}\mathbf{R}_0 &= (\mathbf{R}_{\mathbf{z}}(\phi_i)\mathbf{R}_{\hat{\mathbf{y}}_{1i}}(\alpha_i))^T\end{aligned} \tag{9}$$

Further, ${}^{4i}\mathbf{l}_i$ must be expressed independently for each leg because of the orientation of the local frames (Fig. 3)

$${}^{41}\mathbf{l}_1 = (0 \quad l_1 \quad 0)^T; {}^{42}\mathbf{l}_2 = (0 \quad -l_2 \quad 0)^T;$$
$${}^{43}\mathbf{l}_3 = (0 \quad 0 \quad l_3)^T. \tag{10}$$

Equations (8) are nine equations with nine unknowns: they are ϑ_i, b_i and depending on whether the forward or inverse analysis was dealt with, the position coordinates p_x, p_y, p_z of the reference point P of the moving platform or the actuated displacements a_i, respectively. The first of Eqs. (8) may be

https://doi.org/10.1017/S0263574709005384 Published online by Cambridge University Press

expressed for the ith leg as

$$a_i = c\phi_i c\alpha_i p_x + s\phi_i c\alpha_i p_y - s\alpha_i p_z \tag{11}$$

and putting values of ϕ_i, α_i ($i = 1,2,3$) into the equation, the following relationships may be easily obtained:

$$\begin{aligned} a_1 &= p_x \\ a_2 &= p_y \\ a_3 &= p_z \end{aligned} \tag{12}$$

Equations (12) are linear and fully decoupled. Therefore the input–output relationships, available either for the inverse or the forward kinematics, between a_i and p_x, p_y, p_z, take a surprisingly easy and quick form. Equation (8) provide values of the passive joint variables ϑ_i, b_i as well. Expressing second and third of Eqs. (8) for each leg

Leg1	Leg2	Leg3
$p_y = -b_1 \cdot s\vartheta_1 + l_1$	$p_x = b_2 \cdot s\vartheta_2 + l_2$	$k(p_x - p_y) = -b_3 s\vartheta_3$
$p_z = b_1 \cdot c\vartheta_1$	$p_z = b_2 \cdot c\vartheta_2$	$k(p_x + p_y) = b_3 c\vartheta_3 + l_3$
		$k = 1/\sqrt{2}$

(13)

And manipulating the equations yields to

Leg1	Leg2	Leg3
$\tan\vartheta_1 = -\dfrac{p_y - l_1}{p_z}$	$\tan\vartheta_2 = \dfrac{p_x - l_2}{p_z}$	$\tan\vartheta_3 = \dfrac{k(p_y - p_x)}{k(p_y + p_x) - l_3}$
$b_1 = \dfrac{p_z}{c\vartheta_1}$	$b_2 = \dfrac{p_z}{c\vartheta_2}$	$b_3 = \dfrac{k(p_y - p_x)}{s\vartheta_3}$

(14)

In the forward kinematics the relationships (13) remain the same but replacing p_x, p_y, p_z with a_i ($i = 1,2,3$) because of Eqs. (12).

5. Velocity Analysis, Singularity and Isotropy

Differentiating Eqs. (12) with respect to time and expressing the results in matrix form

$$\dot{\mathbf{a}} = \mathbf{J}\dot{\mathbf{p}} \text{ where } \mathbf{a} = [\dot{a}_1, \dot{a}_2, \dot{a}_3]^T,\ \dot{\mathbf{p}} = [\dot{p}_x, \dot{p}_y, \dot{p}_z]^T. \tag{15}$$

The Jacobian matrix $\mathbf{J}$ is a diagonal matrix, the mechanism does not have any singularity for the translational motion since the determinant of $\mathbf{J}$, det($\mathbf{J}$), is never null and because an identity matrix is a perfectly conditioned matrix, det($\mathbf{J}$) = 1, the present TPM is isotropic in the whole workspace. On the other hand, theoretically, rotational singularities, i.e. constraint singularities, can occur. Let us consider Eq. (2) again. Dot multiplying Eq. (2) by $\hat{\mathbf{n}}_i = \hat{\mathbf{x}}_{1i} \times \hat{\mathbf{y}}_{2i}$

$$\hat{\mathbf{n}}_i \cdot \boldsymbol{\omega} = \hat{\mathbf{n}}_i \cdot (\dot{\vartheta}_i \hat{\mathbf{x}}_{2i} + \dot{\chi}_i \hat{\mathbf{y}}_{3i} + \dot{\lambda}_i \hat{\mathbf{x}}_{4i}) = 0. \tag{16}$$

When system of Eq. (16) becomes singular, $\hat{\mathbf{n}}_1, \hat{\mathbf{n}}_2, \hat{\mathbf{n}}_3$ are linearly dependent and the moving platform is not prevented from rotating yet

$$\det(\mathbf{N}) = \hat{\mathbf{n}}_1 \cdot (\hat{\mathbf{n}}_2 \times \hat{\mathbf{n}}_3) = 0 \tag{17}$$

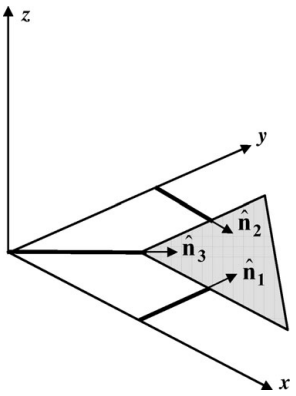


Fig. 4. Constraint singularity configuration.

where $\mathbf{N}$ is

$$\mathbf{N} = \begin{bmatrix} \hat{\mathbf{n}}_1^T \\ \hat{\mathbf{n}}_2^T \\ \hat{\mathbf{n}}_3^T \end{bmatrix} = \begin{bmatrix} 0 & n_{1y} & n_{1z} \\ n_{2x} & 0 & n_{2z} \\ n_{3x} & n_{3y} & 0 \end{bmatrix} \tag{18}$$

$\mathbf{N}$ assumes the form of Eq. (18) since $\chi_i, \dot{\chi}_i \ddot{\chi}_i = 0$ thus $\hat{\mathbf{n}}_i$ coincides with $\hat{\mathbf{z}}_{3i}$. Therefore, constraint singularity occurs only when the moving platform belongs to the xy fixed plane. In this configuration of the TPM $\hat{\mathbf{n}}_1, \hat{\mathbf{n}}_2, \hat{\mathbf{n}}_3$ lie on the same plane (Fig. 4).

6. Numerical Simulation of the Kinematics of the Passive Joints

Given the trajectory of the moving platform, the motions of the passive joints were obtained. The components p_x, p_y, p_z of $\mathbf{p}$ are cubic functions versus time, Eq. (19), whose coefficients were calculated exploiting the motion conditions imposed at the beginning and at the end of the motion, Eq. (20).

$$\begin{aligned} p_x &= p_y = a_0 + a_1 T + a_2 T^2 + a_3 T^3 \\ p_z &= b_0 + b_1 T + b_2 T^2 + b_3 T^3 \\ T &= t/t_F \end{aligned} \tag{19}$$

where t_F is time at the end of the motion. T is called the normalized time.

$$\begin{aligned} &p_x(T=0) = 7.5\,\text{mm} \\ &p_x(T=1) = 10\,\text{mm} \\ &p_z(T=0) = 8.5\,\text{mm} \\ &p_z(T=1) = 15\,\text{mm} \\ &\dot{p}_x(T=0) = \dot{p}_z(T=0) = 0\,\text{mm/s} \\ &\dot{p}_x(T=1) = \dot{p}_z(T=1) = 0\,\text{mm/s} \end{aligned} \tag{20}$$

Passive joints motions were obtained by Eqs. (14), velocities and accelerations were calculated differentiating the positions obtained with respect to time. As example, Eq. (21) provide velocities and accelerations of the passive

https://doi.org/10.1017/S0263574709005384 Published online by Cambridge University Press

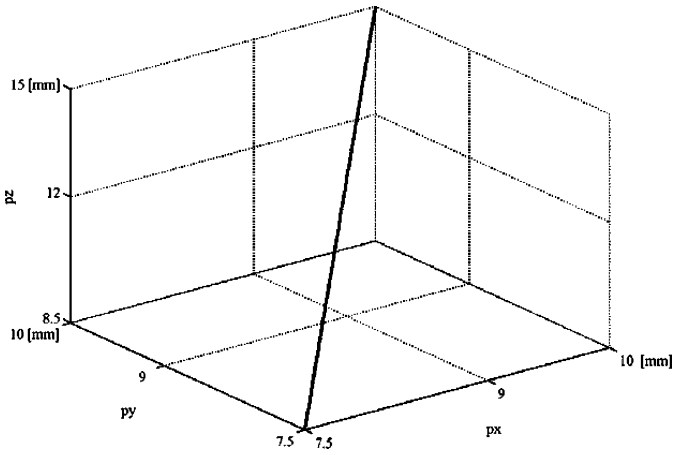


Fig. 5. Trajectory of the reference point P of the moving platform.

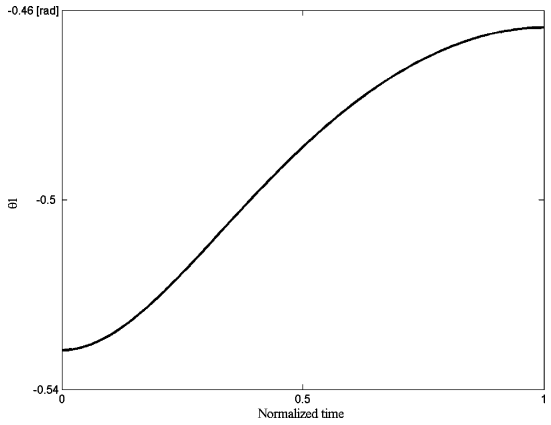


Fig. 6. ϑ_1 versus normalized time.

joints of leg 1

$$\dot{\vartheta}_1 = -\left(\frac{\dot{p}_y + \dot{p}_z \tan\vartheta_1}{(1+\tan^2\vartheta_1)p_z}\right)$$

$$\ddot{\vartheta}_1 = -\left(\frac{\ddot{p}_y + \ddot{p}_z \tan\vartheta_1}{(1+\tan^2\vartheta_1)p_z} + \frac{2\dot{p}_z\dot{\vartheta}_1}{p_z} + 2\tan\vartheta_1\vartheta_1^2\right)$$

$$\dot{b}_1 = \frac{b_1 s\vartheta_1\dot{\vartheta}_1 + \dot{p}_z}{c\vartheta_1}$$

$$\ddot{b}_1 = \tan\vartheta_1(2\dot{b}_1\dot{\vartheta}_1 + b_1\ddot{\vartheta}_1) + b_1\vartheta_1^2 + \frac{\ddot{p}_z}{c\vartheta_1} \qquad (21)$$

In Fig. 5 the trajectory imposed to the reference point P of the moving platform is shown.

Figures 6–9 show, respectively, ϑ_1, $\dot{\vartheta}_1$, b_1 and $\dot{b}_1$ in time.

7. Workspace

Because of the simplicity of the input–output relationships, Eqs. (12), the theoretical workspace, i.e., the locus of points that the reference point P on the moving platform may reach, is directly found to be a parallelepiped of edges a_i. For evaluating the realistic workspace but considering the kinematic limits of each leg, the geometrical approach proposed in ref. [9][9] is adopted. The position of P is calculated independently by means of the kinematics of the ith leg,

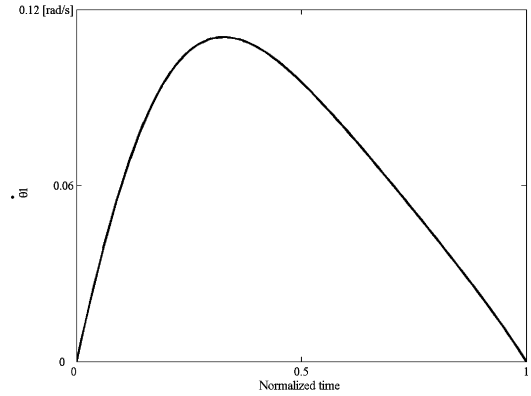


Fig. 7. $\dot{\vartheta}_1$ versus normalized time.

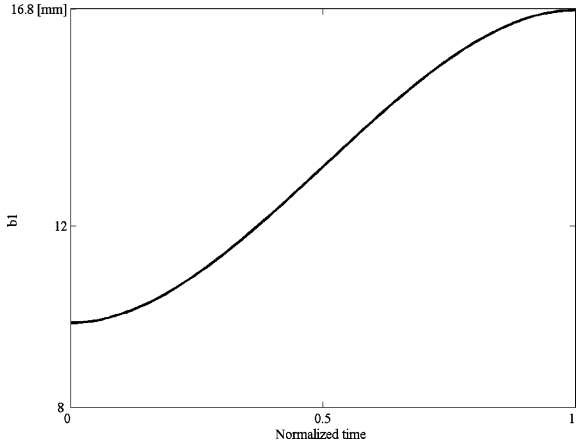


Fig. 8. b_1 versus normalized time.

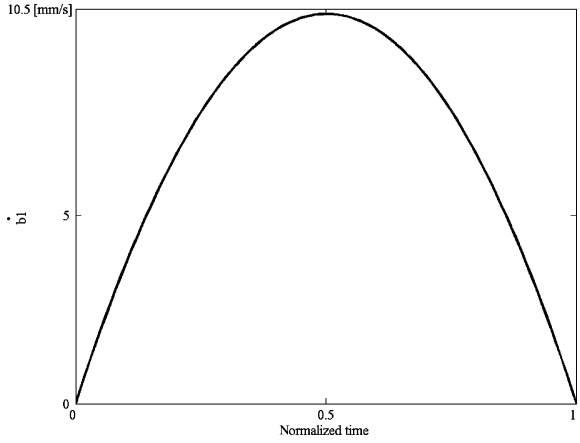


Fig. 9. $\dot{b}_1$ versus normalized time.

then the realistic workspace is calculated as the intersecting volume of the workspace volumes of the legs.

Equations (12) and (13) were necessarily resumed and used for calculating the workspace volume of each leg.

Leg 1	Leg 2	Leg 3
$p_x = a_1$	$p_x = b_2 \cdot s\vartheta_2 + l_2$	$p_x = \dfrac{b_3(c\vartheta_3 - s\vartheta_3) + l_3}{2k}$
$p_y = -b_1 \cdot s\vartheta_1 + l_1$	$p_y = a_2$	$p_y = \dfrac{b_3(c\vartheta_3 + s\vartheta_3) + l_3}{2k}$
$p_z = b_1 \cdot c\vartheta_1$	$p_z = b_2 \cdot c\vartheta_2$	$p_z = a_3$
		$k = 1/\sqrt{2}$

(22)

https://doi.org/10.1017/S0263574709005384 Published online by Cambridge University Press

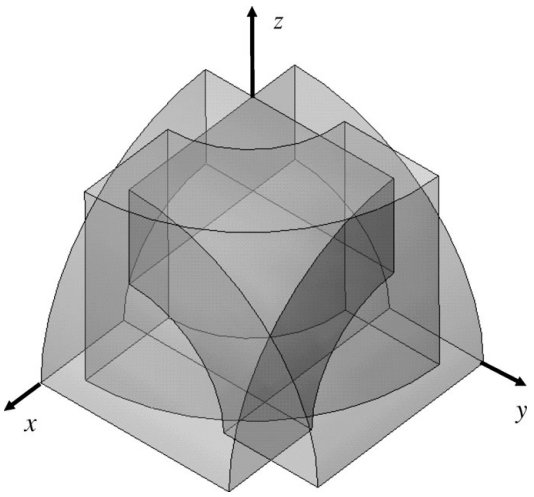


Fig. 10. Intersecting volumes of the PUPR legs.

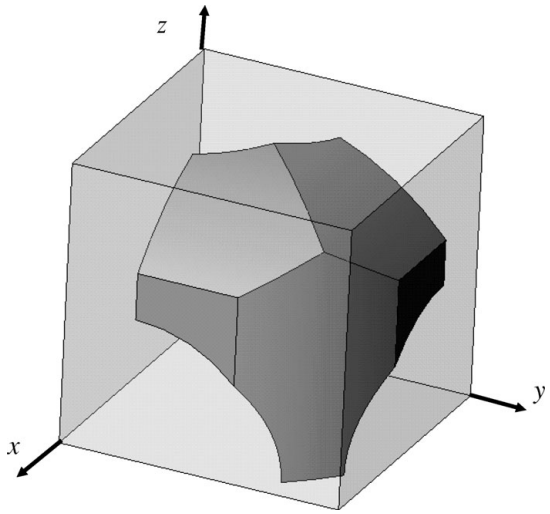


Fig. 11. Workspace of the PUPR by the geometrical approach.

In the computation $0 \le a_i \le a_{\max}$, $0.5a_{\max} \le b_i \le a_{\max}$, $-\pi/2(0) \le \vartheta_1(\vartheta_2) \le 0(\pi/2)$, $-\pi/4 \le \vartheta_3 \le \pi/4$. The characteristic geometrical dimensions of the moving platform $l_1 = l_2 = 0.25a_{\max}$, $l_3 = 0.35a_{\max}$.

From Eqs. (22) it may be noted that b_i is the most significant parameter for the dimensions of the workspace. As clearly shown in Fig. 10 the leg volumes are hollow partial cylinders with axes aligned to the axes of the fixed reference systems. The ith leg volume has an intuitive form, considering that only ϑ_i may change because $\chi_i = 0$ and $\lambda_i = -\vartheta_i$ at all times, thereby guaranteeing that the moving platform is parallel to the fixed base. b_i is the distance between the initial length and the maximum stroke of the passive prismatic pair. The former is the inner radius and the latter is the outer radius of the partial annulus at the leg volume cross section. Figure 11 shows the net volume obtained by intersection, the theoretical workspace is depicted as well. For the chosen dimensions the net workspace is about 50% of the theoretical given by $a_{\max,1} \cdot a_{\max,2} \cdot a_{\max,3}$ and about 85% of the working volume of each leg.

The moving platform may move in the xy plane covering an approximately triangular area being about 1.25% of the theoretical $a_{\max,1} \cdot a_{\max,2}$. This motion must be avoided as it is since affected by constraint singularity, as shown in Section 5 (Fig. 4).

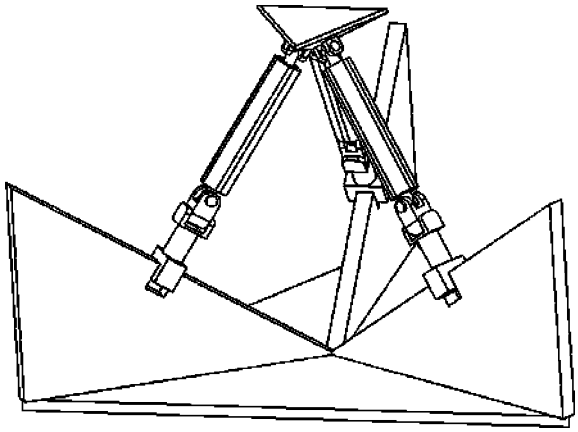


Fig. 12. The PUPR parallel manipulator with $\phi_i = (i-1)\pi/3$, $\alpha_i = \alpha$, $(i = 1,2,3)$.

8. Design and Other Architectures

The design of un-actuated P pairs is a crucial step for a proper performance of the TPM. Indeed, passive prismatic joints may provide friction and even stick-and-slip phenomena that threaten the kinematic and dynamic features of the manipulator. The solution can be to use linear motion guides with recirculating rolling elements, balls or rollers. In this case, friction is drastically reduced and even stick-and-slip may be eliminated thereby preserving stiffness and accuracy of the TPM.

Different architectures of the PUPR manipulator may be found by changing the orientations of the actuated prismatic pairs with respect to the orthogonal architecture proposed so far.

8.1. Alternative architecture 1

A convenient configuration is obtained when $\phi_i = (i-1)\pi/3$, $\alpha_i = \alpha$ $(i = 1,2,3)$, (Fig. 12).

Inverse and forward kinematics are still easy to solve even if the relationships are no longer un-coupled as it happens in the case of the orthogonal setting. Because of their generality, Eq. (8), from the loop vector equation are still available. The first equations provide the inverse kinematics solutions and are explicitly expressed in Eqs. (20):

$$\begin{aligned} a_1 &= c\alpha p_x - s\alpha p_z \\ a_2 &= -c\alpha \left(\frac{p_x - \sqrt{3}p_y}{2} \right) - s\alpha p_z \\ a_3 &= -c\alpha \left(\frac{p_x + \sqrt{3}p_y}{2} \right) - s\alpha p_z \end{aligned} \tag{23}$$

Solution of the forward kinematics is, instead, obtained by manipulating Eqs. (23). Simply subtracting the third equation from the second equation gives p_y. Similarly, by adding the two equations and using the first of Eqs. (23), p_x may

https://doi.org/10.1017/S0263574709005384 Published online by Cambridge University Press

be obtained. Finally, substituting the results into the first equation p_z may be calculated as well.

$$\begin{aligned} c\alpha p_x - s\alpha p_z &= a_1 \\ p_y &= \frac{a_2 - a_3}{\sqrt{3}c\alpha} \\ -c\alpha p_x - 2s\alpha p_z &= -c\alpha p_x - 2(-a_1 + c\alpha p_x) \\ &= a_2 + a_3 \text{ such that } p_x = \frac{2a_1 - a_2 - a_3}{3c\alpha} \\ s\alpha p_z &= -a_1 + \frac{2a_1 - a_2 - a_3}{3} \\ \text{such that } p_z &= -\frac{a_1 + a_2 + a_3}{3s\alpha} \end{aligned} \tag{24}$$

It is easily shown that in this case the manipulator is still isotropic and with no translational singularities. Differentiating Eqs. (23) with respect to time and writing the results in matrix form yields

$$\dot{\mathbf{a}} = \begin{bmatrix} c\alpha & 0 & -s\alpha \\ -\frac{1}{2}c\alpha & \frac{\sqrt{3}}{2}c\alpha & -s\alpha \\ -\frac{1}{2}c\alpha & -\frac{\sqrt{3}}{2}c\alpha & -s\alpha \end{bmatrix} \dot{\mathbf{p}} \tag{25}$$

Here, the Jacobian matrix $\mathbf{J}$ is a constant matrix. Selecting α such that $\mathbf{J}\mathbf{J}^T = \mathbf{I}_{3x3}$, the TPM becomes isotropic in the whole workspace. Therefore

$$\mathbf{J}\mathbf{J}^{\mathbf{T}} = \begin{bmatrix} 1 & 1 - \frac{3c^2\alpha}{2} & 1 - \frac{3c^2\alpha}{2} \\ 1 - \frac{3c^2\alpha}{2} & 1 & 1 - \frac{3c^2\alpha}{2} \\ 1 - \frac{3c^2\alpha}{2} & 1 - \frac{3c^2\alpha}{2} & 1 \end{bmatrix}$$
$$\text{such that } 1 - \frac{3c^2\alpha}{2} = 0 \tag{26}$$

and since negative values of $c\alpha$ make no sense $\alpha = \pm 0.196\pi$. Finally, for selecting which of the two possible angles must be used the determinant of $\mathbf{J}$ may be calculated

$$\det(\mathbf{J}) = 1 = -\frac{3\sqrt{3}}{2}c^2\alpha s\alpha \text{ such that } \alpha = -0.196\pi \tag{27}$$

It is worth noting that if the axes of the prismatic pairs were in a plane, i.e. $\alpha = 0$, $\mathbf{J}$ is singular (i.e. translational singularities). The existence of the constraint singularities may be proved recalling Eqs. (16) and (17). Again the singularity occurs at the limit of the workspace when $\hat{\mathbf{n}}_i$s ($i = 1,2,3$) belong to same plane (Fig. 13).

8.2. *Alternative architecture 2*

A different configuration is obtained when $\phi_i = (i-1)\pi/2$, $\alpha_i = \alpha$ ($i = 1,2,3$). Like it was done for the architecture 1, the kinematic relationships can be written out. Again, the first of Eqs. (8) may be expressed for the three legs as

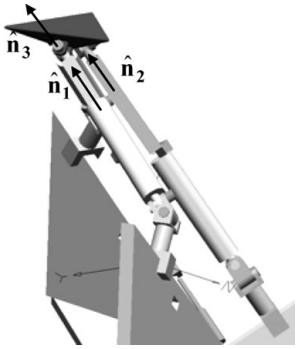


Fig. 13. Constraint singularity configuration with $\phi_i = (i-1)\pi/3$, $\alpha_i = \alpha$, ($i = 1,2,3$).

$$\begin{aligned} a_1 &= c\alpha p_x - s\alpha p_z \\ a_2 &= c\alpha p_y - s\alpha p_z \\ a_3 &= -(c\alpha p_x + s\alpha p_z) \end{aligned} \tag{28}$$

and represent the solution of the inverse position problem. Manipulating Eqs. (28) the relationships solving the forward position problem can be easily found

$$\begin{aligned} p_z &= -\frac{a_1 + a_3}{2s\alpha} \\ p_x &= \frac{a_1 - a_3}{2c\alpha} \\ p_y &= \frac{2a_2 - (a_1 + a_3)}{2c\alpha} \end{aligned} \tag{29}$$

Differentiating Eqs. (28) with respect to time and writing the results in matrix form, the Jacobian matrix can be expressed as

$$\mathbf{J} = \begin{bmatrix} c\alpha & 0 & -s\alpha \\ 0 & c\alpha & -s\alpha \\ -c\alpha & 0 & -s\alpha \end{bmatrix} \tag{30}$$

Also in this case if the axes of the prismatic pairs were in a plane, i.e. $\alpha = 0$, the determinant of $\mathbf{J}$ vanishes, thus the manipulator becomes singular (i.e. translational singularities).

Although $\mathbf{J}$ is constant, it is not possible to select an appropriate α such that the manipulator was isotropic since $\mathbf{J}\mathbf{J}^T \neq \mathbf{I}_{3x3}$ for any α

$$\mathbf{J}\mathbf{J}^T = \begin{bmatrix} 1 & s^2\alpha & -1 + 2s^2\alpha \\ s^2\alpha & 1 & s^2\alpha \\ -1 + 2s^2\alpha & s^2\alpha & 1 \end{bmatrix} \tag{31}$$

8.3. *Design free from singularities*

According to the suggestion of a reviewer of the paper a design of the PUPR manipulator free from constraint singularity can also be proposed. This property is simply obtained by reversing the order of first and second revolute

https://doi.org/10.1017/S0263574709005384 Published online by Cambridge University Press

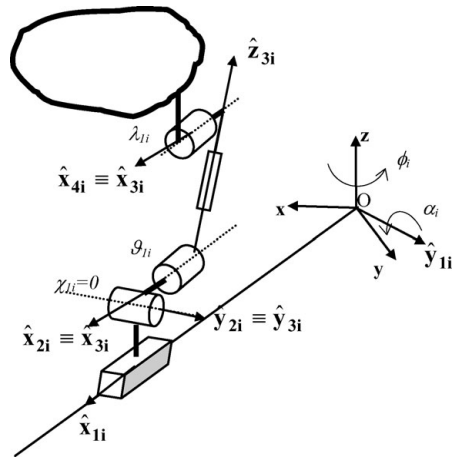


Fig. 14. The ith leg of the PUPR free from constraint singularity.

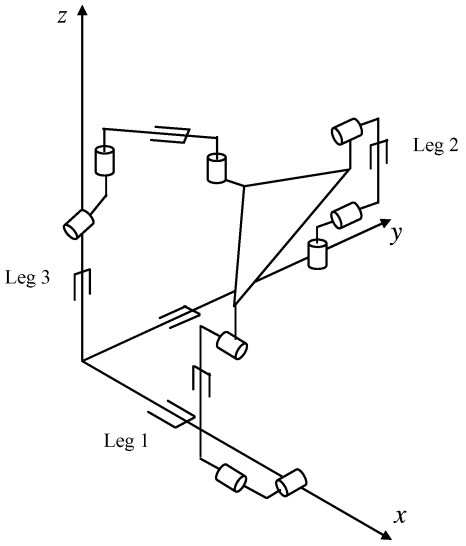


Fig. 15. The design of the PUPR free from constraint singularity.

pair in each leg. Figure 14 shows the leg i of such manipulator. By an identical procedure to that followed in the rest of the paper, it is possible to show that $\chi_i = \dot{\chi}_i = (\vartheta_i + \lambda_i) = (\dot{\vartheta}_i + \dot{\lambda}_i) = 0$ and to find linear relationships between a_i and $\mathbf{p}$. However, in this case, the idle pair is the first R pair in each leg.

Only the absence of the constraint singularity is proved in this section: with reference to the local coordinate reference systems drawn in Fig. 14 for the ith leg, dot multiplying $\boldsymbol{\omega}$ by $\hat{\mathbf{t}}_i = \hat{\mathbf{x}}_{2i} \times \hat{\mathbf{y}}_{3i}$. $\hat{\mathbf{t}}_i$ denotes the perpendicular to the plane formed by the axes of the U pair. Similarly to Eq. (16) it can be written

$$\hat{\mathbf{t}}_i \cdot \boldsymbol{\omega} = \hat{\mathbf{t}}_i \cdot (\dot{\chi}_i \hat{\mathbf{y}}_{2i} + \dot{\vartheta}_i \hat{\mathbf{x}}_{3i} + \dot{\lambda}_i \hat{\mathbf{x}}_{4i}) = 0. \tag{32}$$

In this case $\hat{\mathbf{t}}_1, \hat{\mathbf{t}}_2, \hat{\mathbf{t}}_3$ do not depend on the legs orientation. By a proper configuration of the U axes in each leg, as shown in Fig. 15, $\hat{\mathbf{t}}_1, \hat{\mathbf{t}}_2, \hat{\mathbf{t}}_3$ cannot be linearly dependent

$$\det(\mathbf{T}) = \hat{\mathbf{t}}_1 \cdot (\hat{\mathbf{t}}_2 \times \hat{\mathbf{t}}_3) \neq 0 \tag{33}$$

where $\mathbf{T}$ is

$$\mathbf{T} = \begin{bmatrix} \hat{\mathbf{t}}_1^T \\ \hat{\mathbf{t}}_2^T \\ \hat{\mathbf{t}}_3^T \end{bmatrix} = \begin{bmatrix} 0 & 0 & 1 \\ 1 & 0 & 0 \\ 1/\sqrt{2} & 1/\sqrt{2} & 0 \end{bmatrix} \tag{34}$$

Equations (33) and (34) prove that in this case the manipulator is free from constraint singularity.

9. Conclusion

This paper proposes a novel not-overconstrained TPM, a variant of the 3RRPRR mechanism. A very convenient configuration of the motor axes, forming a right-hand orthogonal tern, provides a surprisingly simple and quick kinematic analysis with fully decoupled linear input–output equations, absence of translational singularities, isotropy in the whole of the workspace. Rotational singularities were found in a very small area at the boundary of the workspace. The realistic workspace is obtained as the intersection of the work–volumes of the legs and, for the range of variation chosen for b_i, it is about 50% of the theoretical workspace.

Other two configurations of the motor axes have been analysed. Considering a $2\pi/3$ angle between the motor axes and for each leg $\alpha_i = \alpha$, the TPM shows a remarkable simplicity in the calculation of the forward, inverse and differential kinematics even if the input–output relationships are no longer un-coupled. Also, the TPM may be assembled such that it is isotropic in the whole of the workspace as soon as an appropriate angle $\alpha = -0.196\pi$ is chosen for the motor axes. Considering a $\pi/2$ angle between the motor axes and for each leg $\alpha_i = \alpha$, the kinematics calculations still show a remarkable simplicity but the TPM cannot be isotropic. Moreover, a design of the PUPR manipulator free from constraint singularity was found by reversing the order of first and second revolute pair in each leg.

There is scope for further work directed to developing kinetostatic relationships and carrying out a structural analysis of the TPM components with the aim of designing and building a prototype of the parallel manipulator assembled in the orthogonal architecture.

Acknowledgments

This research was funded by the Italian Ministry of Research (MIUR). The author would like to thank the peer reviewers of the paper for their helpful comments.

References

1. R. Clavel, "Delta a Fast Robot with Parallel Geometry," *Proceedings of the 18th International Symposium on Industrial Robots*, Sydney Australia (1988) pp. 91–100.
2. P. Wenger and D. Chablat, "Kinematics Analysis of a new Parallel Machine-Tool: The Orthoglide," *Proceedings of ARK*, Piran, France (2000) pp. 305–314.
3. K. E. Neumann, Robot, U.S. Patent 4732525 (Mar. 22, 1988).
4. L. W. Tsai and S. Joshi, "Kinematics and optimization of a spatial 3-UPU parallel manipulator," *ASME J. Mech. Des.* **122**(4), 439–446 (2000).
5. R. Di Gregorio and V. Parenti-Castelli, "A Translational 3-DOF Parallel Manipulator," **In**: *Advances in Robot Kinematics:*

https://doi.org/10.1017/S0263574709005384 Published online by Cambridge University Press

Analysis and Control (J. Lenarčič na and M. L. Husty, eds.) (Kluwer Academic publishers, Dordrecht: The Netherlands, 1998) pp. 49–58.
6. R. Di Gregorio, "Closed-Form Solution of the Position Analysis of the Pure Translational 3RUU Parallel Mechanism," *Proceedings of 8th Symposium on mechanisms and mechanical transmissions*, Timisoara, Romania, Vol. 1 (Oct. 2000) pp. 119–124.
7. M. Carricato and V. Parenti-Castelli, "A Family of 3DOF Translational Parallel Manipulators," *Proceedings of the 2001 ASME Design Engineering Technical Conferences*, Pittsburgh, PA, DAC-21035 (2001).
8. M. Carricato and V. Parenti-Castelli, "Position analysis of a new family of 3-DOF translational parallel manipulators," *ASME J. Mech. Des.* **125**(2), 316–322 (2003).
9. M. Carricato and V. Parenti-Castelli, "Singularity-free fully-isotropic translational parallel mechanisms," *Int. J. Rob. Res.* **21**(9), 161–174 (2002).
10. C. M. Gosselin, X. Kong, S. Foucault and I. A. Bonev, "A Fully Decoupled 3-DOF Translational Parallel Mechanism," *Proceedings of the 4th Chemnitz Parallel Kinematics Seminar, Parallel Kinematic Machines International Conference*, Chemnitz: Germany (2004) pp. 595–610.
11. C. M. Gosselin and X. Kong, "Kinematics and singularities analysis of a novel type of 3-CRR 3-dof translational parallel manipulator," *Int. J. Rob. Res.* **21**(9), 791–798 (Sep. 2002).
12. J. M. Hervé, "Design of Parallel Manipulators via the Displacement Group," *Proceedings of the 9th World Congress on the Theory of Machines and Mechanisms*, Milan, Italy (1995) pp. 2079–2082.
13. X. Kong and C. M. Gosselin,"Type synthesis of 3-DOF translational parallel manipulators based on screw theory," *J. Mech. Des.* **126**(1), 83–92 (2004).
14. X. Kong and C. M. Gosselin, "Type Synthesis of Linear Translational Parallel Manipulators," **In**: *Advances in Robot Kinematics: Theory and Applications* (J. Lenarcic and F. Thomas, eds.) (Kluwer Academic Publishers, 2002) pp. 453–462.
15. A. Frisoli, D. Checcacci, F. Salsedo and M. Bergamasco, "Synthesis by Screw Algebra of Translating In-Parallel Actuated Mechanisms," *Advances in Robot Kinematics* (J. Lenarčič and M. M. Stanišić, eds.) (Kluwer Academic publishers, 2000) pp. 433–440.
16. S. Staicu and D. Zhang, "A novel dynamic modelling approach for parallel mechanisms analysis," *Rob. Comput. -Integr. Manuf.* **24**, 167–172 (2008).
17. S. Staicu, X.-J. Liu and J. Wang, "Inverse dyanamics of the HALF parallel manipulator with revolute actuators," *Nonlinear Dyn.* **50**, 1–12 (2007).

https://doi.org/10.1017/S0263574709005384 Published online by Cambridge University Press